Eur. Phys. J. D **11**, 167–173 (2000)

THE EUROPEAN PHYSICAL JOURNAL D

EDP Sciences

Energy levels and optical oscillator strengths of inner-shell excited states and photoionizations of the ground and first excited states of C IV ion

J. Zeng, J. Yuan[a], Z. Zhao, and Q. Lu

Department of Applied Physics, National University of Defense Technology, Changsha 410073, P.R. China

Received 29 September 1999 and Received in final form 8 December 1999

Abstract. Extensive configuration interaction wave functions are determined to calculate the energies of the inner-shell excited states and the oscillator strengths of the optically allowed inner-shell transitions of C IV ion. Photoionization cross-sections of the ground and the first excited states of C IV ion are also obtained by using the R-matrix method. The positions of some inner-shell excited states are redetermined more accurately by analyzing the resonance structures of the photoionization processes. Some of the results are compared with other available theories and experiments.

PACS. 32.70.Cs Oscillator strengths, lifetimes, transition moments – 32.80.Hd Auger effect and inner-shell excitation or ionization – 32.80.Fb Photoionization of atoms and ions

1 Introduction

The energy levels, oscillator strengths and photoionization cross-sections are the basic parameters of atoms. They have many applications in plasma physics, Laser physics, astrophysics, and opacity calculations. Up to now, the energy levels and oscillator strengths of valence-electron transitions have been studied extensively, but relatively less knowledge have been obtained, either from experiment or from calculation, for the inner-electron transitions or photoionizations of the multiply-charged ion. However, data about such processes are required for the understanding of plasmas and astrophysical phenomena [1,2]. They are also of considerable importance for the interpretation of properties of solids since atoms in condensed matter matrices most often exist in ionic forms [3].

While many theoretical and experimental studies have been published about the C IV ion, relatively fewer data have been reported for the inner-shell and doubly excited states. Most theoretical calculations have been focused on lower principal quantum numbers. Yan Gongjing *et al.* [4] calculated the energy levels of valence-electron excited states and transition probabilities of C IV with the principal quantum number less than 4. Biemont [5], Martin and Wiese [6], and Lindgard and Nielsen [7] have reported oscillator strength calculations of C IV. Peach, Saraph and Seaton [8], Drew and Storey [9], and McGuinness, Bell and Hibbert [10] have calculated the photoionization cross-sections of C IV, and the last two include the inner-shell photoionization. The inner-shell spectrum of carbon has been studied by Gabriel [11], who calculated energies of some doubly excited states of the type $1s2l2l'$. Burke [12] has calculated the Stark broadening parameters and collision strengths of C IV by using the R-matrix method. More recently, Jannitti *et al.* [13], and Jannitti *et al.* [14] have reported $1s$ electron absorption spectra of carbon ion obtained with the two laser-produced plasma technique. From the measured $1s$ inner-electron absorption spectra, one can determine the energies of inner-shell excited states.

The purpose of this paper is to calculate the energies of the inner-shell excited states and the optical oscillator strengths of transitions between the low-lying states and the inner-shell excited states of C IV. For completeness, we also give some results related to the valence-shell excitations. The calculations involve extensive configuration interaction (CI), in addition to the configuration representing the main spectroscopic label of the state, to incorporate correlation effects. Then we calculate the photoionization cross-sections of the ground and first excited states of C IV with more attention putted on the analysis of the resonance structures. By determining the positions of the related resonances, we can obtain the energies of the inner-shell excited states more accurately. The calculations show that this is an effective method of obtaining the energies of the inner-shell excited states. The calculated results are compared with the K-shell photoabsorption spectra obtained by Jannitti *et al.* [14].

2 Method of calculation

We have calculated the energies and oscillator strengths of C IV ion by using the general configuration interaction

[a] e-mail: jmyuan@nudt.edu.cn

code CIV3 [15]. The CI wave functions take the form

$$\Psi(\gamma J) = \sum a_i \Phi_i(\alpha_i L_i S_i J) \tag{1}$$

where the configuration state functions $\{\Phi_i\}$ are associated with a total spin and orbital angular momentum, which are coupled with J. The $\{\alpha_i\}$ denotes state labels such as orbital occupancy and angular momentum coupling schemes of the orbitals. γ denotes a further label for each level, typically the orbital occupancy and S, L of the dominant configuration (with the largest $|a_i|$) although in some cases the mixing between the $\{\Phi_i\}$ is so strong that such labeling is not particularly meaningful.

The one-electron orbitals from which the $\{\Phi_i\}$ are constructed take the form

$$u(X, m_s) = \frac{1}{r} P_{nl}(r) Y_{m_l}(\theta, \phi) \chi_{m_s}(\sigma) \tag{2}$$

and the radial functions are written as sums of Slater-type orbital

$$P_{nl}(r) = \sum C_{jnl} r^{I_{jnl}} \exp(-\zeta_{jnl} r) \tag{3}$$

where we require

$$\int P_{nl}(r) P_{n'l}(r) \mathrm{d}r = \delta_{nn'}; \quad (l < n' \leq n) \tag{4}$$

so that the orbitals form an orthonormal set.

The parameters of the radial functions are determined variationally by minimizing specific eigenvalues of a non-relativistic (LS-coupled) Hamiltonian matrix. In the present calculations, we have optimized 16 radial functions: $2p$, $3s$, $3p$, $3d$, $4s$, $4p$, $4d$, $4f$, $5s$, $5p$, $5d$, $6s$, $6p$, $6d$, $7s$, $7p$. $1s$, $2s$ functions are chosen to be HF functions given by Clementi and Roetti [16] for the ground state $1s^2 2s\ ^2\mathrm{S}$ of C IV.

The wave functions in the form (1) for the C IV ion are used to calculate the absorption oscillator strengths, in both length (f_l) and velocity (f_v) forms. For the transitions from an initial state Ψ_i to a final state Ψ_f

$$f_\mathrm{l} = \frac{2\Delta E}{3 g_\mathrm{i}} \mid \langle \Psi_\mathrm{i} \mid \sum_{p=1}^{N} \mathbf{r}_p \mid \Psi_\mathrm{f} \rangle \mid \tag{5}$$

$$f_\mathrm{v} = \frac{2}{3 g_\mathrm{i} \Delta E} \mid \langle \Psi_\mathrm{i} \mid \sum_{p=1}^{N} \boldsymbol{\nabla}_p \mid \Psi_\mathrm{f} \rangle \mid, \tag{6}$$

where $\Delta E = E_\mathrm{f} - E_\mathrm{i}$, E_i and E_f are, respectively, the energies of initial and final states and $g_\mathrm{i} = (2L_\mathrm{i}+1)(2S_\mathrm{i}+1)$ is the statistical weight of the lower state.

The R-matrix method has been discussed in great detail by Burke *et al.* [17]. The present calculations have been carried out by using the latest Belfast atomic R-matrix code [18]. In an R-matrix calculation, the wave function of the $N+1$ electron system is given the form

$$\Psi_k(X_1 ... X_{N+1}) = \hat{A} \sum_{ij} c_{ijk} \Phi_\mathrm{i}(X_1 ... X_N \widehat{\mathbf{r}}_{N+1} \sigma_{N+1}) u_{ij}(r_{N+1}) + \sum_j d_{jk} \phi_j(X_1 .... X_{N+1}), \tag{7}$$

where $\widehat{A}$ is the antisymmetrization operator to take the exchange effect between the target electrons and the free electron into account. X_i stands for spatial ($\mathbf{r}_\mathrm{i}$) and the spin (σ_i) coordinates of the ith electron. The square integrable orbitals are cast as linear combinations of Slater-type orbitals of equation (3). The parameters ζ_{jnl} and coefficients C_{jnl} are determined by a variational optimization on the energy of a particular state, whilst the powers of r and I_{jnl} remain fixed. Ten orbitals ($1s$, $2s$, $2p$, $3s$, $3p$, $3d$, $4s$, $4p$, $4d$, $4f$) are included in the calculation of photoionizations. The R-matrix boundary is chosen to be 8.4 a.u. As for the construction of the continuum states, each of the angular momentum orbitals is expressed as a linear combination of 20 numerical basis functions. In forming the $(N+1)$-electron configurations in equation (7), all possible excitations of the $2s$-valence electron and a $1s$-core electron into any of the valence orbitals are allowed for. Five C V target states are utilized. They are $1s^2\ ^2\mathrm{S}$, $1s2s\ ^{3,1}\mathrm{S}$, $1s2p\ ^{3,1}\mathrm{P}^o$.

3 Results and discussions

Using the method described above, we calculated the energies for the valence excited and inner-shell excited states and the oscillator strengths of inner-electron and valence-electron transitions of C IV. In order to get enough CI terms, only one electron is kept to stay in $1s$ orbital, the other two are distributed freely among the orbitals. In Table 1 the energies for the valence excited and inner-shell excited states of C IV are presented together with the experimental values and the recent theoretical calculation of Burke [12]. The second column is the present CIV3 results, with the upper part being the energies of the valence excited states and the lower part being that of inner-shell excited states. The third column is the positions of the resonances appearing in the photoionizations, which will be discussed later. The next one is the experimental data. The experimental energy levels of singly excited states are taken from Moore [19], and the inner-shell excited states from Jannitti *et al.* [14]. Jannitti *et al.* measured the $1s$ inner-electron absorption spectrum of the C IV ion with the two laser-produced plasma technique. The absorption was due to the transitions from $1s$ to np, so the experimental results were for $^2\mathrm{P}^o$ states. Quite good agreement is found between the present CIV3 calculations and the experimental energies for the valence and inner-shell excited states. It can be seen that the relative difference of calculated and experimental values of the energy levels of all the valence excited states are less than 0.35% except for the $2p\ ^2\mathrm{P}^o$ state (0.5%), which is slightly better than that of Burke [12] for the first few low-lying states. For the inner-shell excited states, the relative difference is less than 0.88% for wherever the experimental results are available. The third column is the energies obtained by resonance structure analysing, which will be discussed later.

Table 2 shows the oscillator strengths of valence-electron transitions: $^2\mathrm{S}$–$^2\mathrm{P}^o$, $^2\mathrm{P}^o$–$^2\mathrm{S}$, $^2\mathrm{P}^o$–$^2\mathrm{D}$ for $n \leq 7$. Length and velocity forms are given so as to access the

Table 1. Energies of valence-shell and inner-shell excited states of C IV (in *Ry*).

Terms	Present CIV3	Resonances	Experiment	Burke
$(1s^2)2s\ ^2$S	0.0		0.0[a]	0.0
$2p\ ^2$P^o	0.5933		0.5883	0.5931
$3s\ ^2$S	2.7534		2.7598	2.7522
$3p\ ^2$P^o	2.9116		2.9167	2.9097
$3d\ ^2$D	2.9526		2.9606	2.9511
$4s\ ^2$S	3.6498		3.6573	3.6477
$4p\ ^2$P^o	3.7142		3.7209	3.7116
$4d\ ^2$D	3.7309		3.7393	3.7292
$5s\ ^2$S	4.0503		4.0585	
$5p\ ^2$P^o	4.0823		4.0903	
$5d\ ^2$D	4.0915		4.0997	
$6s\ ^2$S	4.2637		4.2717	
$6p\ ^2$P^o	4.2818		4.2899	
$6d\ ^2$D	4.2941		4.2954	
$7s\ ^2$S	4.3938		4.3983	
$7p\ ^2$P^o	4.4016		4.4099	
$1s2s^2\ ^2$S	21.5173	21.420		
$1s2p^2\ ^2$S	23.1853	23.033	22.98[b]	
$1s2s(^3$S$)3s\ ^2$S	24.8251	24.638		
$1s2s(^1$S$)3s\ ^2$S	25.0406	24.924		
$1s2s(^3$S$)4s\ ^2$S	25.7376	25.518		
$1s2s(^1$S$)4s\ ^2$S	25.8403	25.726		
$1s2s(^3$S$)5s\ ^2$S	26.0693	25.963		
$1s2s(^1$S$)5s\ ^2$S	26.1869			
$1s2s(^3$S$)6s\ ^2$S	26.3886			
$1s2s(^3$S$)2p\ ^2$P^o	22.1360	22.035	22.04	
$1s2s(^1$S$)2p\ ^2$P^o	22.4749	22.306	22.30	
$1s2s(^3$S$)3p\ ^2$P^o	24.8754	24.710	24.72	
$1s2s(^1$S$)3p\ ^2$P^o	25.1944	25.060	25.13	
$1s2s(^3$S$)4p\ ^2$P^o	25.8727	25.630	25.65	
$1s2s(^1$S$)4p\ ^2$P^o	26.1361	26.050	26.08	
$1s2s(^3$S$)5p\ ^2$P^o	26.2117	26.100	26.12	
$1s2s(^1$S$)5p\ ^2$P^o	26.5339	26.449	26.48	
$1s2s(^3$S$)6p\ ^2$P^o	26.4245	26.307	26.32	
$1s2s(^1$S$)6p\ ^2$P^o	26.7404		26.65	
$1s2s(^3$S$)7p\ ^2$P^o	26.5488	26.542		
$1s2p^2\ ^2$P	22.7235		22.63	
$1s2p^2\ ^2$D	22.6771	22.526	22.63	
$1s2s(^3$S$)3d\ ^2$D	25.0698	24.891		
$1s2s(^1$S$)3d\ ^2$D	25.3318	25.204		
$1s2s(^3$S$)4d\ ^2$D	25.8726	25.745		
$1s2s(^1$S$)4d\ ^2$D	26.1701	26.114		
$1s2s(^3$S$)5d\ ^2$D	26.2387	26.165		
$1s2s(^1$S$)5d\ ^2$D	26.5449			
$1s2s(^3$S$)6d\ ^2$D	26.5678			

[a] Ref. [19], [b] Ref. [14]

Table 2. Oscillator strengths of valence-electron transitions for C IV.

Transitions	$f_{\rm l}$	$f_{\rm v}$	Burke
$2s-2p$	0.2915	0.3073	0.2928
$2s-3p$	0.1999	0.1972	0.1986
$2s-4p$	0.0612	0.0592	0.0592
$2s-5p$	0.0266	0.0258	
$2s-6p$	0.0145	0.0140	
$2s-7p$	0.0088	0.0084	
$2p-3s$	0.0370	0.0392	0.0373
$3s-3p$	0.4850	0.4969	0.4855
$3s-4p$	0.2017	0.1999	0.1998
$3s-5p$	0.0637	0.0636	
$3s-6p$	0.0288	0.0302	
$3s-7p$	0.0150	0.0168	
$2p-4s$	0.0065	0.0074	0.0068
$3p-4s$	0.0819	0.0828	0.0815
$4s-4p$	0.6678	0.6672	0.6703
$4s-5p$	0.2105	0.2072	
$4s-6p$	0.0735	0.0692	
$4s-7p$	0.0368	0.0324	
$2p-5s$	0.0022	0.0028	
$3p-5s$	0.0154	0.0156	
$4p-5s$	0.1292	0.1270	
$5s-5p$	0.8458	0.8501	
$5s-6p$	0.2257	0.2306	
$5s-7p$	0.0713	0.0768	
$2p-6s$	0.0009	0.0015	
$3p-6s$	0.0062	0.0063	
$4p-6s$	0.0255	0.0251	
$5p-6s$	0.1773	0.1816	
$6s-6p$	0.9984	1.0827	
$6s-7p$	0.2563	0.2313	
$2p-3d$	0.6492	0.6489	0.6512
$2p-4d$	0.1222	0.1218	0.1231
$2p-5d$	0.0444	0.0441	
$2p-6d$	0.0875	0.0835	
$3p-3d$	0.0410	0.0584	0.0585
$3p-4d$	0.5426	0.5419	0.5421
$3p-5d$	0.1301	0.1281	
$3p-6d$	0.1743	0.1788	
$3d-4p$	0.0165	0.0164	
$4p-4d$	0.1010	0.1080	0.1012
$4p-5d$	0.5123	0.5026	
$4p-6d$	0.3706	0.3513	
$3d-5p$	0.0032	0.0031	
$4d-5p$	0.0397	0.0395	
$5p-5d$	0.1512	0.1806	
$5p-6d$	1.0970	0.9044	

wave functions. We also include the calculated values based on R-matrix close-coupling method obtained recently by Burke [12] for comparison. One can see that the agreement is reasonably good, the relative differences between our length and velocity forms being less than 5% for most transitions. For the transitions of $ns\ ^2$S–$n'p\ ^2$P^o, the oscillator strengths are larger and the agreement of length and velocity forms is better when $\Delta n = n' - n = 0, 1$ is satisfied than in other cases. Take $2s-np$ transitions as examples. For $2s-2p$ and $2s-3p$, the relative differences between the length and velocity forms are 2.3% and 1.4% respectively. While for $2s-4p$, $2s-5p$, $2s-6p$ and $2s-7p$, the relative differences are 3.3%, 3.3%, 3.4%, and 4.7%, respectively. For transitions of $np\ ^2$P^o–$n'd\ ^2$D, similar conclusion can be drawn for the cases of $\Delta n = n' - n = 1, 2$. From Tables 1 and 2, we conclude that the wave functions we obtained are very good, and thus the energy levels and oscillator strengths are reliable.

Table 3 shows the oscillator strengths of inner-electron transitions $1s^22s\ ^2$S$-1s2s(^{3,1}$S$)np\ ^2$P^o and $1s^22p\ ^2$P$^o-1s2s(^{3,1}$S$)nd\ ^2$D in C IV, together with the relative values to the oscillator strength of the first transition $1s^22s\ ^2$S–$1s2s(^{3,1}$S$)2p\ ^2$P^o in length and velocity forms. The agreement between the length and velocity forms is also reasonably satisfactory. The relative values show the basic trends of the two series: the oscillator strengths of transitions from the ground state $1s^22s\ ^2$S to the two Rydberg series $1s2s(^{3,1}S)np\ ^2$P^o decrease with the principal quantum number n. This can be understood qualitatively by the general trends of oscillator strengths [20]. For a Rydberg series of spectrum lines, among other factors, such as transition energies and angular momentum, the oscillator strengths and the effective quantum numbers $n_{\rm f}$ approximately have the following relation

$$f_{\rm l}(n_i l_i \gamma JM - n_j l_j \gamma\prime J') \propto (n_j^*)^{-3}.$$

So with the increase of the principal quantum number n the oscillator strengths decrease quite fast. For the two transition of $1s^22s\ ^2$S–$1s2s(^3$S$)2p\ ^2$P^o and $1s^22s\ ^2S$–$1s2s(^1$S$)2p\ ^2$P^o, the oscillator strength of the former is much larger than the latter, although the configuration of the final state is the same ($1s2s2p$). This difference may be accounted for by the angular momentum portion. The different angular momentum couplings make them differing considerably.

In order to test the reliability of our CIV3 results, we performed a five-state close-coupling calculation for the ground and first excited states of C IV. From the resonance structures of photoionizations, we can determine the positions of the inner-shell excited states, and thus their energies more accurately. For the ground state ^{2}S of C IV, there is only one kind of allowed final channel ^{2}P^o. Figure 1 shows the general behaviour of the photoionization cross-section of the ground state of C IV. The ground state ionization potential derived for C IV is $-4.7363Ry$, differing by about 0.1% from the observed energy of $-4.7421Ry$, which are the relative energy to the ground state of C V target. From the inspection of Figure 1, it can be seen that the photoionization cross-section

Table 3. Oscillator strengths of inner-shell transitions for C IV.

Transitions	f_l	relative values	f_v	relative values
$(1s^2)2s\ ^2\mathrm{S}-1s2s(^3\mathrm{S})2p\ ^2\mathrm{P}^o$	0.4784	1.000	0.4438	1.000
$(1s^2)2s\ ^2\mathrm{S}-1s2s(^3\mathrm{S})3p\ ^2\mathrm{P}^o$	0.0635	0.133	0.0567	0.128
$(1s^2)2s\ ^2\mathrm{S}-1s2s(^3\mathrm{S})4p\ ^2\mathrm{P}^o$	0.0308	0.064	0.0272	0.061
$(1s^2)2s\ ^2\mathrm{S}-1s2s(^3\mathrm{S})5p\ ^2\mathrm{P}^o$	0.0106	0.022	0.0088	0.020
$(1s^2)2s\ ^2\mathrm{S}-1s2s(^3\mathrm{S})6p\ ^2\mathrm{P}^o$	0.0065	0.014	0.0054	0.012
$(1s^2)2s\ ^2\mathrm{S}-1s2s(^3\mathrm{S})7p\ ^2\mathrm{P}^o$	0.0031	0.006	0.0023	0.005
$(1s^2)2s\ ^2\mathrm{S}-1s2s(^1\mathrm{S})2p\ ^2\mathrm{P}^o$	0.0583	1.000	0.0556	1.000
$(1s^2)2s\ ^2\mathrm{S}-1s2s(^1\mathrm{S})3p\ ^2\mathrm{P}^o$	0.0355	0.609	0.0322	0.579
$(1s^2)2s\ ^2\mathrm{S}-1s2s(^1\mathrm{S})4p\ ^2\mathrm{P}^o$	0.0073	0.125	0.0066	0.119
$(1s^2)2s\ ^2\mathrm{S}-1s2s(^1\mathrm{S})5p\ ^2\mathrm{P}^o$	0.0038	0.065	0.0035	0.063
$(1s^2)2s\ ^2\mathrm{S}-1s2s(^1\mathrm{S})6p\ ^2\mathrm{P}^o$	0.0014	0.024	0.0015	0.027
$(1s^2)2s\ ^2\mathrm{S}-1s2s(^1\mathrm{S})7p\ ^2\mathrm{P}^o$	0.00063	0.011	0.00075	0.013
$(1s^2)2p\ ^2\mathrm{P}^o-1s2p^2\ ^2\mathrm{D}$	0.1384		0.1308	
$(1s^2)2p\ ^2\mathrm{P}^o-1s2s(^3\mathrm{S})3d\ ^2\mathrm{D}$	0.0050		0.0044	
$(1s^2)2p\ ^2\mathrm{P}^o-1s2s(^1\mathrm{S})3d\ ^2\mathrm{D}$	0.0029		0.0024	
$(1s^2)2p\ ^2\mathrm{P}^o-1s2s(^3\mathrm{S})4d\ ^2\mathrm{D}$	0.0009		0.0007	
$(1s^2)2p\ ^2\mathrm{P}^o-1s2s(^1\mathrm{S})4d\ ^2\mathrm{D}$	0.0000		0.0001	

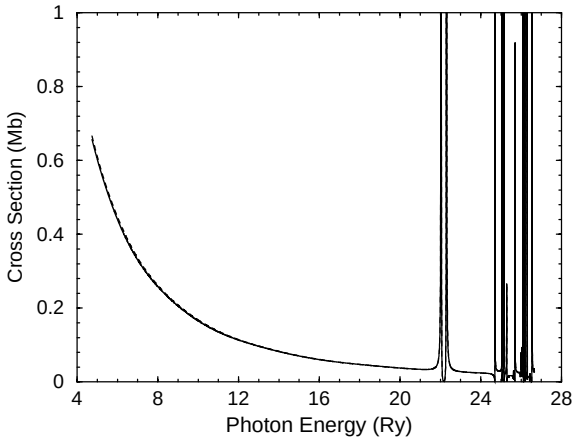

Fig. 1. The total photoionization cross-section of the ground state of C IV. Solid line refers to the length form, dashed one to the velocity form.

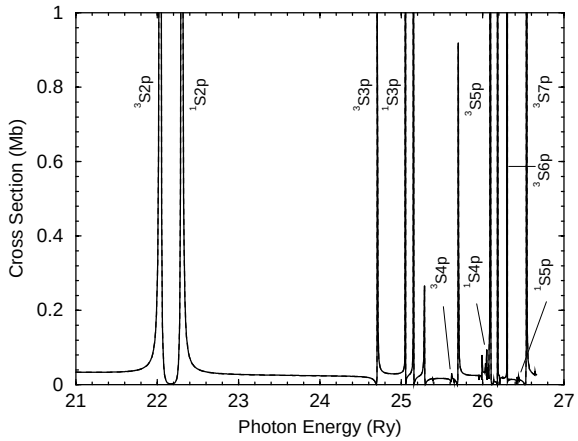

Fig. 2. The same as in Figure 1, but expanded to show the resonance structures more clearly. The labels are on the left sides of corresponding resonances except that indicated by lines and $1s2s(^1\mathrm{S})2p\ ^2\mathrm{P}^o$ and $1s2s(^3\mathrm{S})7p\ ^2\mathrm{P}^o$, the later two are on the right for convenience.

first decreases monotonously from the ionization threshold to about $21.6Ry$, then exhibits complicated resonance structures. In order to see clearly the resonance structures, an expansion is given in Figure 2. Below the first and second excitation threshold, we have identified the resonance series to be $1s2s(^{3,1}\mathrm{S})np\ ^2\mathrm{P}^o$ Rydberg series. The corresponding energies of the resonances are tabulated in the third column in Table 1. Excellent agreement is obtained between the calculated and experimental results. The relative differences are less than 0.3%, most of which are about 0.1%. This also proves that our calculated results are reliable.

For the photoionization of the first excited state $1s^22p\ ^2\mathrm{P}^o$ of C IV, there are three allowed final channels ^{2}S, ^{2}P and ^{2}D according to the selection rule. The total cross-section is the sum of the three partial ones. The partial waves ^{2}S and ^{2}D have contribution from the first ionization threshold $4.1467Ry$, while the partial wave ^{2}P opens from the fourth ionization threshold $1s2p\ ^3\mathrm{P}^o$, *i.e.* $26.5197Ry$. So we only give the partial cross-sections of the first two partial waves. Figure 3 shows the partial cross-sections of: (a) $^2\mathrm{P}^o$–^{2}S and (b) $^2\mathrm{P}^o$–^{2}D. For brevity, we do not give the total cross-section. The energy step is $0.0002Ry$ to show the resonance structures. The solid lines refer to the length form and the dashed lines to velocity form. From the inspection of Figures 3a and 3b one can see that close agreement is found between the

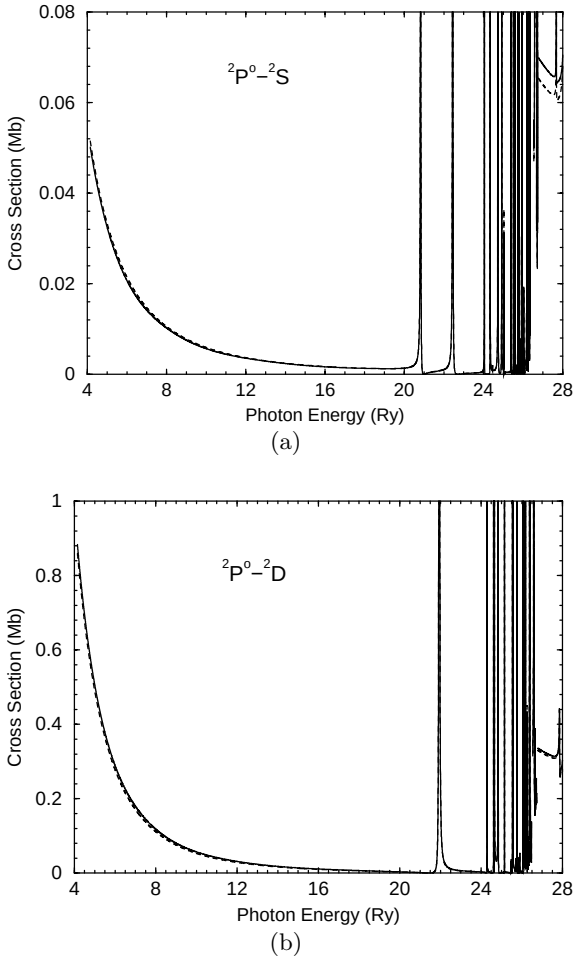

Fig. 3. The meaning of the lines are the same as in Figure 1, but for the partial cross-sections of: (a) ^{2}S and (b) ^{2}D for the first excited state $1s^2 2p\ ^2P^o$.

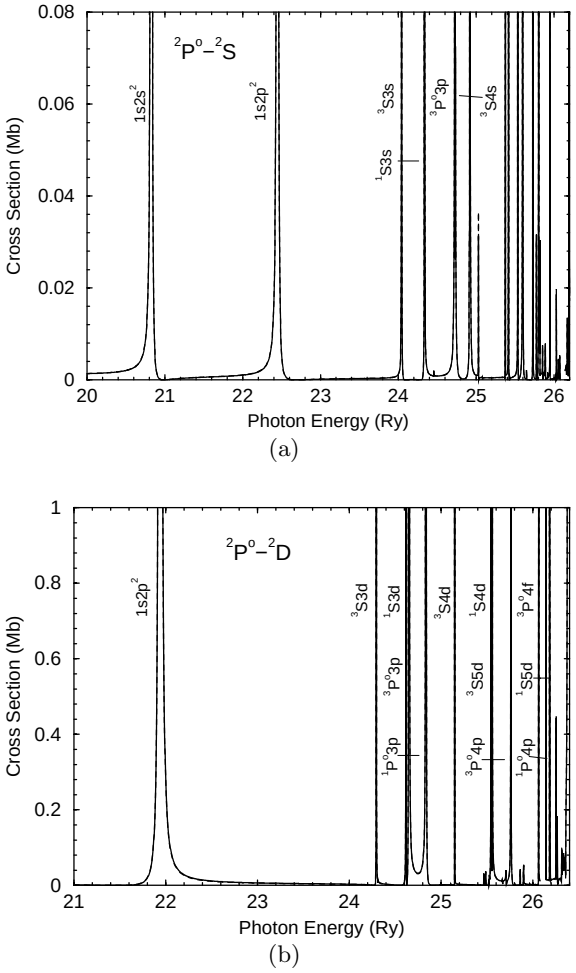

Fig. 4. (a) and (b) are, respectively, the same as (a) and (b) in Figure 3, but to show the resonance structures in an expanded scale. The labels are on the left sides of corresponding resonances except that indicated by lines. Please be noted that in (a) the resonances of $1s2p(^3P^o)3p\ ^2$S and $1s2s(^3S)4s\ ^2$S, and in (b) the resonances of $1s2p(^3P^o)3p\ ^2$D and $1s2s(^1S)3d\ ^2$D, are so close that they can not be seen clearly.

length and velocity forms. This agreement is needed in photoionization calculations. The dominant contribution comes from $^2P^o$–^{2}D partial cross-section in most photon energy range, except in the range of 19–21.6Ry the contribution from ^{2}S partial cross-section is larger than ^{2}D. The partial cross-sections exhibit complicated resonance structures. They are dominated by the autoionizing resonances belonging to different Rydberg series. We have analyzed these Rydberg series. For brevity, we only give some results of the ^{2}S, ^{2}D partial cross-sections near the threshold in Figures 4a and 4b. From the identification of Rydberg series, one can obtain the resonance energy, and hence the energies of inner-shell excited states.

For partial ^{2}S, the first resonance is caused by the autoionizing state $1s2s^2\ ^2$S, the second one by the autoionizing state $1s2p^2\ ^2$S. Some other resonances are shown in Figure 4a. They are caused by the following Rydberg series: $1s2s(^3S)n's\ ^2$S, $1s2s(^1S)n's\ ^2$S, $1s2p(^3P^o)n'p\ ^2$S, and $1s2p(^1P^o)n'p\ ^2$S. For ^{2}D partial wave, the first resonance is caused by the autoionizing state $1s2p^2\ ^2$D, the others by the following Rydberg series: $1s2s(^3S)n'd\ ^2$D, $1s2s(^1S)n'd\ ^2$D, $1s2p(^3P^o)n'p\ ^2$D, $1s2p(^1P^o)n'p\ ^2$D, $1s2p(^3P^o)n'f\ ^2$D, and $1s2p(^1P^o)n'f\ ^2$D. The results are also tabulated in the third column in Table 1. Excellent agreement is obtained for the inner-shell excited states between our results and the observed values of Jannitti [14]. For example, the relative error for the inner-shell excited states $1s2p^2\ ^2$D, ^{2}S are 0.02% and 0.3% respectively.

In the Figures 2 and 4, one can see that there are several series of autoionizing resonances and the widths of them differ widely within a series. This can be understood from the viewpoint of multichannel quantum defect theory (MQDT) [21]: for a Rydberg series of autoionizing resonances, the widths of resonances are proportional to the square of the coupling matrix elements between the autoionizing Rydberg states and the ionization channel and in inverse proportion to the cube of the effective quantum number n^* of the autoionizing state.

The decrease of the widths of the autoionizing resonances within a series with the principal quantum numbers n is clearly demonstrated in Figures 2 and 4 for the labeled Rydberg series of autoionizing resonances. For example, in Figure 2, the first two states $(1s2s)\ ^3\mathrm{S}2p$ and $(1s2s)\ ^1\mathrm{S}2p$ of the two labelled series have the largest widths because of their smallest effective quantum numbers. With the increasing of n, the widths become more and more narrower. With the same configuration but different symmetries, for examples, $1s2p^2\ ^2\mathrm{D}$ and $1s2p^2\ ^2\mathrm{S}$, the widths of resonance structures have the same order. So the autoionizing widths are more dependent on the effective quantum numbers than on the coupling matrix elements.

In conclusion, we have calculated the wave functions, energies, oscillator strengths of the inner-shell excited states and photoionization cross-sections of the ground and first excited states in C IV, with the emphasis on the energies of the inner-shell excited states. Good agreements among the CIV3 results, the results determined by the resonance positions of the R-matrix calculations, and the experiments show that our results are reliable.

This work was supported by the National Science Foundation of China under Grant No. 19504002, the Science Foundation of China Academy of Engineering Physics under Grant No. 95009, and China Research Association of Atomic and Molecular Data (CRAAMD).

References

1. N.R. Simon, Astrophys. J. **260**, L87 (1982).
2. W.H. Parkinson, in *Spectroscopy of Astrophysical Plasmas*, edited by A. Dalgarno, D. Layzer (Cambridge University Press, Cambridge, 1987), p. 302.
3. L.C. Davis, J. Appl. Phys. **59**, R25 (1986); B. Hermsmeier, C.S. Fadley, M.O. Krause, J. Jimenez-Mier, P. Gerard, S.T. Mansin, Phys. Rev. Lett. **61**, 2592 (1988).
4. Yan Gongjing, Zhou Zhongyuan, Pan Shoupu, Chin. J. At. Mol. Phys. **15**, 527 (1998) (*in Chinese*).
5. E. Biemont, Astron. Astrophys. Suppl. **27**, 489 (1977).
6. G.A. Martin, W.L. Wiese, J. Phys. Chem. Ref. Data **5**, 537 (1976).
7. A. Lindgard, S.E. Nielsen, At. Data Nucl. Data Tables **19**, 533 (1977).
8. G. Peach, H.E. Saraph, M.J. Seaton, J. Phys. B **21**, 3669 (1988).
9. J.E. Drew, P.J. Storey, J. Phys. B **15**, 2357 (1982).
10. C. McGuinness, K.L. Bell, A. Hibbert, J. Phys. B **30**, 59 (1997).
11. A.H. Gabriel, Mon. Not. R. Astr. Soc. **160**, 99 (1972).
12. V.M. Burke, J. Phys. B **25**, 4917 (1992).
13. E. Jannitti, P. Nicolosi, G. Tondello, Phys. Scripta **41**, 458 (1990).
14. E. Jannitti, P. Nicolosi, P. Villoresi, F. Xianping, Phys. Rev. A **51**, 314 (1995).
15. A. Hibbert, Comput. Phys. Commun. **9**, 141 (1975).
16. E. Clementi, C. Roetti, At. Data Nucl. Data Tables **14**, 177 (1974).
17. P.G. Burke, A. Hibbert, W.D. Robb, J. Phys. B **4**, 153 (1971).
18. K.A. Berrington, W.B. Eissner, P.H. Norrington, Comput. Phys. Commun. **92**, 290 (1995).
19. *Atomic Energy Levels*, edited by C.E. Moore, Nat. Bur. Stand. U.S. Title Series No. I (U.S. GPO, Washington, D.C., 1970), p. 21.
20. R.D. Cowan, *Theory of Atomic Spectra* (University of California Press, Berkeley, 1981), p. 436.
21. Harald Friedrich, *Theoretical Atomic Physics* (Springer-Verlag, 1990), p. 146.